Eur J Nutr (2018) 57:391–403
DOI 10.1007/s00394-017-1433-z

ORIGINAL CONTRIBUTION

Myricetin-induced brown adipose tissue activation prevents obesity and insulin resistance in db/db mice

Tao Hu[1,2] · Xiaoxue Yuan[2] · Gang Wei[2] · Haoshu Luo[3] · Hyuek Jong Lee[2,4] · Wanzhu Jin[2]

Received: 22 September 2016 / Accepted: 5 March 2017 / Published online: 24 April 2017

Abstract
Purpose Myricetin, a dietary flavonoid, is effective in the treatment of obesity and insulin resistance by increasing glucose transport and lipogenesis in adipocyte and diminishing systemic inflammation in obesity. However, it has not been revealed yet whether myricetin is associated with brown adipose tissue (BAT) activation that tightly mediates systemic energy metabolism. Therefore, this study assessed whether myricetin activated brown adipose tissue in db/db mouse.
Methods Myricetin (400 mg/kg) in distilled water was fed daily by oral gavage to leptin receptor-deficient db/db male mice at 4 weeks of age for 14 weeks. Body weight change, glucose intolerance test, blood lipid profile and BAT activation using PET-CT were assessed.
Results After myricetin treatment for 14 weeks, systemic insulin resistance and hepatic steatosis were significantly improved in db/db mice with body weight reduction and myricetin led to decreased adipocity, improved plasma lipid profiles and increased energy expenditure. Myricetin activated BAT by upregulating thermogenic protein expression and activating mitochondrial biogenesis, eventually increasing heat dissipation in skin after cold exposure. In iWAT, myricetin induced beige formation, increased thermogenic protein expression and activated mitochondrial biogenesis. Consistently, thermogenic gene expression was upregulated when myricetin was introduced in $C_3H_{10}T_{1/2}$ cells during brown adipocytes differentiation. Moreover, the expression level of adiponectin was significantly increased in $C_3H_{10}T_{1/2}$ cells, adipose tissues and plasma after myricetin treatment.
Conclusions These results highlight that myricetin prevents obesity and systemic insulin resistance by activating BAT and increasing adiponectin expression in BAT.

Keywords Myricetin · Brown adipose tissue · Inguinal white adipose tissue · Obesity

Abbreviations

BAT	Brown adipose tissue
iWAT	Inguinal white adipose tissue
PGC1-α	Peroxisome proliferator-activated receptor gamma coactivator 1-alpha
PGC1-β	Peroxisome proliferator-activated receptor gamma coactivator 1-beta
UCP1	Uncoupling protein-1
CHO	Cholesterol
TG	Triacylglyceride

Electronic supplementary material The online version of this article (doi:10.1007/s00394-017-1433-z) contains supplementary material, which is available to authorized users.

✉ Haoshu Luo
luohaoshu@cau.edu.cn

✉ Hyuek Jong Lee
Hyuekjong.lee@gmail.com

✉ Wanzhu Jin
jinw@ioz.ac.cn

[1] Department of Anatomy, Basic Medical College, Xuzhou Medical University, Xuzhou, Jiangsu 221004, People's Republic of China

[2] Key laboratory of Animal Ecology and Conservation Biology, Institute of Zoology, Chinese Academy of Sciences, Beijing 100101, People's Republic of China

[3] State key Laboratory of Agrobiotechnology, Department of Animal Physiology, College of Biological Sciences, China Agricultural University, Beijing 100193, People's Republic of China

[4] Present Address: Center for Vascular Research, Institute for Basic Science (IBS), Daejeon 34141, Republic of Korea

LDL	Low-density lipoprotein
HDL	High-density lipoprotein
ATP5A	ATP synthase, H + transporting, mitochondrial F1 complex, alpha 1
UQCRC2	Cytochrome b-c1 complex subunit 2
SDHB	Succinate dehydrogenase [ubiquinone] iron–sulfur subunit, mitochondrial
SIRT1	NAD-dependent deacetylase sirtuin-1
GAPDH	Glyceraldehyde 3-phosphate dehydrogenase
TH	Tyrosine hydroxylase
dio2	Dopamine and iodothyronine deiodinase types 2
TBX1	T-box transcription factor TBX1
TMEM26	Transmembrane protein 26

Introduction

The prevalence of obesity is associated with adverse health outcomes such as type 2 diabetes, fatty liver disease, stroke, cardiovascular diseases, and certain types of cancer [1, 2]. The pharmacological approaches to the treatment of obesity have been focused on reducing food absorption and/or depressing appetite. Now, Food and Drug Administration (FDA) recommends only five drugs (orlistat, phentermine/topiramate, bupropion/naltrexone, liraglutide, and lorcaserin) for obese patients [3]. However, pharmacological treatment for obesity can cause side effects including headache, insomnia, nausea and respiratory infections and its outcome has not been satisfied yet [3].

Since it had been reported that human adults have functional BAT [4–6], BAT activation has received great attention as an alternative therapeutic option for the treatment of obesity and insulin resistance (IR) due to its importance on energy metabolism. BAT is characterized by multilocular lipid droplets and higher number of mitochondria that uncouples fuel oxidation from ATP to generate heat [7]. BAT is the main organ to produce non-shivering thermogenesis (NST) and maintain whole-body temperature [8]. Multiple lines of evidence have demonstrated that cold-induced NST reverses obesity and improves insulin sensitivity by activating BAT [9, 10]. Recently, our group demonstrated that BAT transplantation suppresses body weight gain and ameliorates IR by activating endogenous BAT in obese mice [11, 12]. Furthermore, we also reported that BAT transplantation ameliorates anovulation, hyperandrogenism and polycystic ovary with an improvement of IR in polycystic ovary syndrome (PCOS) that is a complex endocrinopathy [13]. In addition, BAT activity has a negative correlation with BMI and the percentage of body fat [5, 14] highlighting an important role of BAT in energy balance.

As a third type of adipocyte, brown adipocytes in white adipose tissue (WAT), called brite/beige cells, are recruited in WAT by cold exposure or β3-adrenoceptor agonist treatment and they express uncoupling protein-1 (UCP1), one of the specific markers of brown adipocyte [15]. The gene signatures of beige cells have a similarity with those of classical BAT rather than WAT [15] and the recruitment of beige cells in WAT also increases energy metabolism, leading to the improvement of metabolic disorders [16, 17]. Therefore, activation of brown adipocytes and beige formation may provide a new promising strategy for clinical application to treat obesity and metabolic diseases.

Myricetin is a dietary flavonoid that is abundant in plants such as berries, tea, fruits, wines and vegetables [18]. Myricetin has various biological functions including antioxidant, cytoprotective, antiviral, antimicrobial, anti-inflammatory, and antiplatelet activities [19]. Additionally, myricetin stimulates glucose transport in rat adipocytes and enhances insulin-stimulated lipogenesis [20]. Moreover, myricetin treatment ameliorates hyperglycemia in diabetic rat [20], and normalizes the carbohydrate metabolic products and renal function markers in streptozotocin and cadmium-induced diabetic nephrotoxic rats [21]. Recently, it has been reported that myricetin improves IR in diet-induced obese mouse by diminishing the level of serum inflammatory cytokines [22]. Although BAT activation is commonly associated with the reduction of body fat, it has not been studied yet whether myricetin has BAT activation-mediated anti-obesity effect.

In the present study, we revealed that myricetin activated BAT in db/db mice. Consequently, myricetin protected against body weight gain without change of diet consumption and improved IR, glucose tolerance and hepatic steatosis in db/db mice. In addition, myricetin also induced beige formation in inguinal white adipose tissue (iWAT). Collectively, our results show that myricetin-mediated BAT activation and beige formation contribute to the improvement of adverse metabolic phenotypes in db/db mice.

Materials and methods

Mice

C57BLKS/J-Leprdb/Leprdb (db/db) male mice were purchased from the Biomedical Research Institute of Nanjing University. Mice were housed under constant environmental condition in the Office of Laboratory Animal Welfare-certified animal facility with a 12-hour light–dark cycle. Food and water were provided ad libitum. Mice were treated with myricetin (400 mg/kg, Aladdin Inc, Shanghai, China) in distilled water daily by oral gavage from 4 weeks of age for 14 weeks ($N = 10$) [23]. Control mice (Cont) were treated with same volume of vehicle (distilled water) daily by oral gavage from 4 weeks of age for 14 weeks

($N = 10$). After 14 weeks of treatment, mice were killed and then BAT and iWAT were snap frozen in liquid nitrogen and stored at −80 °C for molecular analysis or formalin fixed for histologic analyses. Ethical approval was obtained for all animal procedures from the Institutional Animal Care and Use Committee of Institute of Zoology, Chinese Academy of Sciences and all procedures complied with the NIH Guide for the Care and Use of Laboratory Animals.

Body composition

Mice were weighed every week. At 18 weeks of age, body composition was analyzed by a desktop NMR analyzer (MesoQMR 23-060H-I, Niumag Corporation, China) according to the manufacturer's instruction.

Metabolic assessment

For glucose tolerance tests (GTT), mice were fasted for 16 h (17:00–9:00) with free access to drinking water. Blood glucose level was determined using an Accu-Chek glucose monitor (Roche Diagnostics Corp, Pleasanton, CA, USA) immediately before, 15, 30, 60 and 120 min after intra-peritoneal glucose injection (1.0 g/kg). For insulin tolerance test (ITT), mice were fasted for 4 h (9:00–13:00) and human insulin (0.8 units/kg, Humulin; Eli Lilly) was injected intraperitoneally. Blood glucose level was determined immediately before, 15, 30, 45 and 60 min after insulin injection.

Oxygen consumption and physical activity

Metabolic rate was measured by indirect calorimetry with an open flow system (Sable, FoxBox, North Las Vegas, USA) as described previously [24]. Briefly, mice were adapted to the system for 20–24 h and then VO_2 and VCO_2 were measured during next 24 h. Heat production and RER were calculated as described previously [11]. Voluntary activity of each mouse was measured using optical beam technique (Opto-M3; Columbus Instruments, Columbus, OH, USA) over 24 h and was expressed as 24-h average activity. During measurement, mice were maintained at 24 °C under 12-h light/dark cycle with free access to food and water.

Positron emission tomography-computed tomography (PET-CT)

PET/CT imaging was acquired with the Siemens Inveon Dedicated PET (DPET) System and Inveon Multimodality (MM) System (CT/SPECT) (Siemens Preclinical Solutions, Knoxville, TN, USA) at the Institute of Laboratory Animal Sciences, Chinese Academy of Medical Sciences. Before the experiment, the db/db mice were fasted overnight and then each mouse was anesthetized with isoflurane. Subsequently, each mouse was injected with about 800 mCi ^{18}F-FDG intravenously. The db/db mice were subjected to PET/CT analysis 1 h after the ^{18}F-FDG injection using Inveon Acquisition Workplace (IAW) software. A 10-min CT X-ray for attenuation correction was scanned with a power of 80 kv and 500 mA and an exposure time of 1100 ms before the PET scan. After that, PET scan was performed within the remaining 10 min. The images were reconstructed with the three-dimensional ordered-subsets expectation maximum (OSEM). The three-dimensional regions of interest (ROIs) were drawn over the guided CT images and the ^{18}F-FDG absorption rate was expressed as the percent of the injected dose per gram of body weight (%ID/g) using Inveon Research Workplace (IRW) (Siemens) software. We quantified BAT activity using the standardized uptake value (SUV), which was determined by dividing the relevant ROI concentration by the ratio of the injected activity to the body weight.

Core body temperature and infrared thermography

Mice were exposed to cold chamber (6 °C) for up to 4 h with free access to food and water. The rectal probe connected to digital thermometer (Yellow Spring Instruments, Yellow Spring, OH, USA) was used to measure the core body temperature after cold exposure. Skin temperature was measured by the infrared digital thermographic camera (E60: Compact Infrared Thermal Imaging Camera; FLIR; West Malling, Kent, UK) and images were analyzed using the FLIR Quick Report software (FLIR ResearchIR Max 3.4; FLIR; West Malling).

Plasma lipid profile

After euthanization with Avertin (240 mg/kg, Sigma, USA), blood was taken from heart and then plasma was collected to detect the level of cholesterol (CHO), triacylglyceride (TG), low-density lipoprotein (LDL) and high-density lipoprotein (HDL) using ELISA kits (NanJing Jian Cheng Bioengineering Institute).

Histologic analysis and immunohistochemistry

Tissues were fixed with 4% paraformaldehyde overnight at room temperature and then embedding and sectioning were performed. Sections with 5-μm thickness were stained with hematoxylin and eosin (H&E) then images were acquired by microscope (DS-RI1, Nikkon, JP). The mean area of 50–100 random adipocytes from each animal was calculated as previously described [25]. To detect neutral lipid, cryo-sectioned liver tissue was stained with 0.2%

(w/v) Oil-Red O (Sigma–Aldrich, St. Louis, MO, USA) for 10 min at RT after fixation. For UCP1 staining, tissue specimens were deparaffinized, boiled in sodium citrate buffer (10 mM sodium citrate, 0.05% Tween 20, pH 6.0) for 20 min, blocked with 5% normal goat serum for 60 min, incubated with anti-UCP1 antibody (1:400 dilution; Santa Cruz Biotechnologies) at 4 °C overnight and then incubated with the HRP-conjugated secondary antibody for 1 h at room temperature. UCP1 signal was detected with DAB kit (ZSGB-BIO, Beijing, China) according to the manufacturer's instruction and images were acquired by microscope (DS-RI1, Nikkon, JP).

RNA isolation and gene expression analysis

Total RNA was extracted from BAT and iWAT using TRIzol isolation reagent (Invitrogen, Carlsbad, CA) according to the manufacturer's instruction. RNA concentration was spectrophotometrically determined using NanoDrop (Thermo Scientific). Two microgram of RNA from tissue was reverse transcribed using murine leukemia virus reverse transcriptase and oligo (dT)16 primer. The resulting cDNAs from tissue samples were assayed in duplicate. qRT-PCR was conducted using 2X SYBR green PCR master mix on a real-time PCR system (Applied Biosystems). Gene expression data was normalized to the housekeeping gene cyclophilin A and analyzed using the delta delta cycle threshold method ($\Delta\Delta C_t$) [26]. Primer sets are described in supplementary Table 1.

Western blot analysis

Tissues were dissolved in RIPA buffer [150 mM sodium chloride, 1.0% TritonX-100, 0.5% sodium deoxycholate, 0.1% SDS, 50 mM Tris, protease and phosphatase inhibitor cocktail (Roche Diagnostics Corp, Pleasanton, CA, USA)]. Protein concentrations were determined using a BCA assay kit (Pierce Diagnostics Corp, Pleasanton, CA, USA). Protein was separated by 10 or 15% SDS-PAGE, transferred to PVDF membrane (Millipore Billerica, MA, USA), blocked in 5% skim milk in TBST (0.02 M Tris base, 0.14 M Nacl, 0.1% Tween 20, pH 7.4), incubated with primary antibodies for overnight at 4 °C and then incubated with secondary antibodies conjugated with HRP. Signals were detected with Super Signal West Pico Chemiluminescent Substrate (Pierce, Rockford, IL, USA) and were visualized and analyzed by densitometric scanning (Image Quant TL7.0, GE healthcare Bio-Sciences AB). Primary antibodies used in this study are anti-UCP1 (1:1000, Abcam), anti-OXPHOS (1:250, Abcam), anti-Sirt1 (1:1000, Abcam), anti-PGC1α (1:1000, Abcam), anti-GAPDH (1:1000, Cell Signaling Technology) and anti-tubulin (1:1000, Abcam).

Mitochondrial DNA (mtDNA) content quantification by quantitative real-time PCR

Total DNA (genomic and mtDNA) was isolated from tissues using TIANamp Genomic DNA Kit (TIANGEN BIOTECH, China) according to the manufacturer's protocol. DNA concentration was spectrophotometrically determined using NanoDrop (Thermo Scientific). Quantitative real-time PCR was used to analyze the mtDNA copy number. COX-II was used as a mitochondrial genome marker gene and β-globin was used as a nuclear marker gene. Primer sequences are listed in supplementary Table 1.

Cell culture

Cell culture products and most other biochemical reagents were purchased from Sigma-Aldrich (St. Louis, MO, USA), unless otherwise specified. $C_3H_{10}T_{1/2}$ cells, the mouse mesenchymal stem cell line, were purchased from National Platform of Experimental Cell Resources (Sci-Tech, Shanghai, China). $C_3H_{10}T_{1/2}$ cells were grown to confluence in differentiation medium supplemented with 10% FBS, 850 nM insulin and 1 nM 3,3′,5-triiodo-L-thyronine (T3) and then brown adipocytes differentiation was induced with differentiation medium supplemented with 10% FBS, 0.5 mM isobutylmethylxanthine, 0.5 mM dexamethasone, 0.12 mM indomethacin, 850 nM insulin, 1 nM T3 for 2 days. After 2 days of induction period, cells were changed back to differentiation medium with vehicle (water) or myricetin (10 uM) for 6 days [27]. After 6 days of differentiation, fully differentiated brown adipocytes were used for subsequent analysis.

Statistics

All results are expressed as means ± standard deviation (SD) using Prism software. To test normality, the Shapiro–Wilk test was performed and then, depending its outcome, data were analyzed with using the Student's *t* test, one-way ANOVA with Turkey's post hoc tests or two-way ANOVA with Sidak's multiple comparison test (body weight change, GTT and ITT). Statistical significance was set at $P < 0.05$.

Results

Myricetin suppresses body weight gain in db/db mice

To investigate whether myricetin prevents body weight gain, male db/db mice at 4 weeks of age were orally treated with vehicle or myricetin for 14 weeks. Myricetin-treated db/db mice did not gain as much body

weight as control mice (Fig. 1a). This difference in body weight gain between groups emerged at 9 weeks after myricetin treatment (54.34 ± 1.41 vs 50.25 ± 0.75 g, $p < 0.05$) and the biggest difference was found at 14 weeks after treatment (59.60 ± 1.34 vs 51.18 ± 1.16 g, $p < 0.0001$). To analyze the change of adiposity after myricetin treatment, body composition was measured with NRM analyzer. Total body fat mass of myricetin-treated mice decreased ~27% compared with that of control mice (Fig. 1b). However, there was no change in diet consumption (Fig. 1c) between groups, suggesting that myricetin does not effect on appetite of db/db mice. Morphologically, the size of adipocytes observed on H&E-stained tissue sections was smaller in BAT and iWAT from myricetin-treated mice than control mice (Fig. 1d) and iWAT included higher number of smaller adipocytes after myricetin treatment (Fig. 1e). These results indicate that myricetin suppresses body weight gain by reducing adiposity in db/db mice.

Myricetin prevents metabolic dysfunction in db/db mice

Db/db mice develop obesity-induced hyperlipidemia, fatty liver and IR [28]. Therefore, we tested whether myricetin-mediated fat reduction prevented IR and liver steatosis in db/db mice. The results from GTT showed that plasma glucose level at 15, 60 and 90 min after glucose injection and the value of area under the curve (AUC) were significantly decreased in myricetin-treated mice than in control mice (Fig. 2a, b). ITT and AUC further supported the significant improvement of insulin sensitivity after myricetin treatment (Fig. 2c, d). In addition, histological analysis of liver sections after H&E and Oil-Red-O staining showed the dramatic attenuation of lipid accumulation within liver from myricetin-treated mice (Fig. 2e), suggesting that myricetin treatment could prevent hepatic steatosis. Concomitantly, plasma levels of CHO and LDL were significantly decreased and HDL was significantly increased in myricetin-treated mice (Table 1). However, the plasma level of triglyceride (TG) was comparable between groups (Table 1). Taken together, these results demonstrate that myricetin prevents IR, attenuates hepatic steatosis and improves lipid

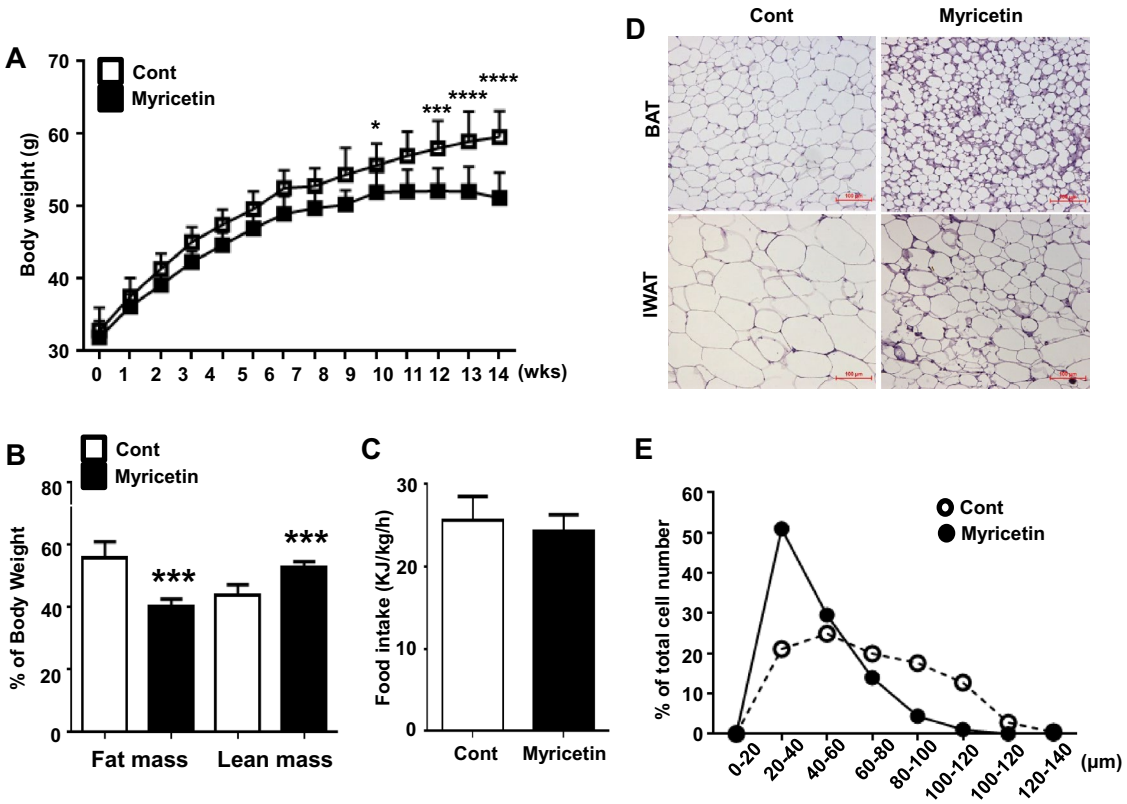

Fig. 1 Myricetin treatment attenuates body weight gain in db/db mice. Vehicle or myricetin were daily administrated for 14 weeks. Myricetin treatment significantly decreases body weight gain (**a**) and body fat mass (**b**) without change of diet consumption between groups (**c**). Representative histologic images of H&E-stained BAT and iWAT (**d**). Percentage of different size of adipocyte cells in iWAT (**e**). A *graph* and *bars* represent means ± SD. ($N = 10$). Data analyzed by two-way ANOVA with Sidak's multiple comparison test (A) $^{*}P < 0.05$, $^{**}P < 0.01$, $^{***}P < 0.001$, $^{****}P < 0.0001$ vs Cont

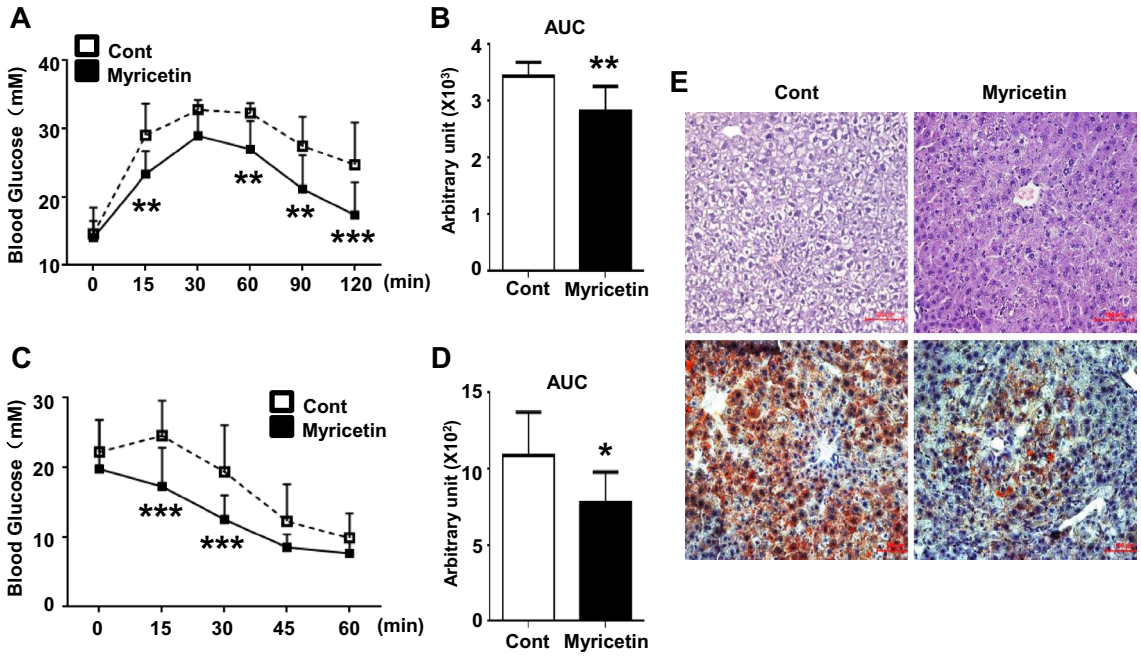

Fig. 2 Myricetin prevents metabolic dysfunction in db/db mice. GTT (**a**) and ITT (**c**) were performed at 9 and 10 weeks after vehicle or myricetin treatment, respectively ($N=9$–10). *Bar graphs* represent AUCs for GTT (**b**) and ITT (**d**). Representative histologic images of H&E stained and Oil-Red O stained liver (**e**). *Graphs* and *bars* represent means ± SD. Data analyzed by two-way ANOVA with Sidak's multiple comparison test (**a, c**) $^{*}P<0.05$, $^{**}P<0.01$, $^{***}P<0.001$ vs Cont

Table 1 Plasma lipid changes after myricetin treatment

	Control	Myricetin
CHO (mmol/L)	2.11 ± 0.163	1.50 ± 0.229*
TG (mmol/L)	1.62 ± 0.375	1.19 ± 0.090
LDL (mmol/L)	0.31 ± 0.057	0.17 ± 0.023*
HDL (mmol/L)	1.77 ± 0.161	2.22 ± 0.107*

All values represent means ± SD

CHO cholesterol, *LDL* low-density lipoprotein, *HDL* high-density lipoprotein, *TG* triglyceride

*$P<0.05$ vs Cont

profiles, positively regulating whole body energy metabolism and glucose homeostasis in db/db mice.

Myricetin increases energy expenditure in db/db mice

We next investigated whether myricetin treatment increases energy expenditure in db/db mice using indirect calorimetry (TSE labmaster system), since decreased energy expenditure is one of predominant phenotypes of db/db mice [29]. After 24-h acclimation in chamber at 24 °C, VO_2 and VCO_2 were measured for next 24 h under 12-h light/dark cycle with free access to food and water. Notably, oxygen consumption during 24 h and mean oxygen consumption were significantly increased in myricetin-treated mice (Fig. 3a, b). Therefore, whole body mean energy expenditure was increased in myricetin db/db mice (Fig. 3c). To analyze whether increased oxygen consumption after myricetin treatment is mediated by increased physical activity, spontaneous physical activity of each mouse was measured for 24 h. However, there was no difference in physical activity between groups (Fig. 3d). These results suggest that increased energy expenditure by myricetin treatment is not associated with physical activity.

Myricetin activates BAT in db/db mice

It is well established that BAT activation increases energy expenditure [30]. Therefore, we hypothesized that myricetin may increase energy expenditure by activating BAT in db/db mouse. To test our hypothesis, BAT activity was assessed with PET-CT. PET-CT images showed that ^{18}F-FDG uptake of BAT located within the dashed triangle was ~3 times higher in myricetin-treated mice than control mice (Fig. 4a, b), indicating that myricetin activates BAT in db/db mice. For further analysis, mice were placed in thermo-neutral (30 °C) and cold (6 °C) environments for 6 h and then core body temperature was measured. At thermoneutral (30 °C) environment, there was no change in average core body temperature between groups. However, it was significantly higher in myricetin-treated mice after 6 h of cold exposure (Fig. 4d). Infrared thermographic images

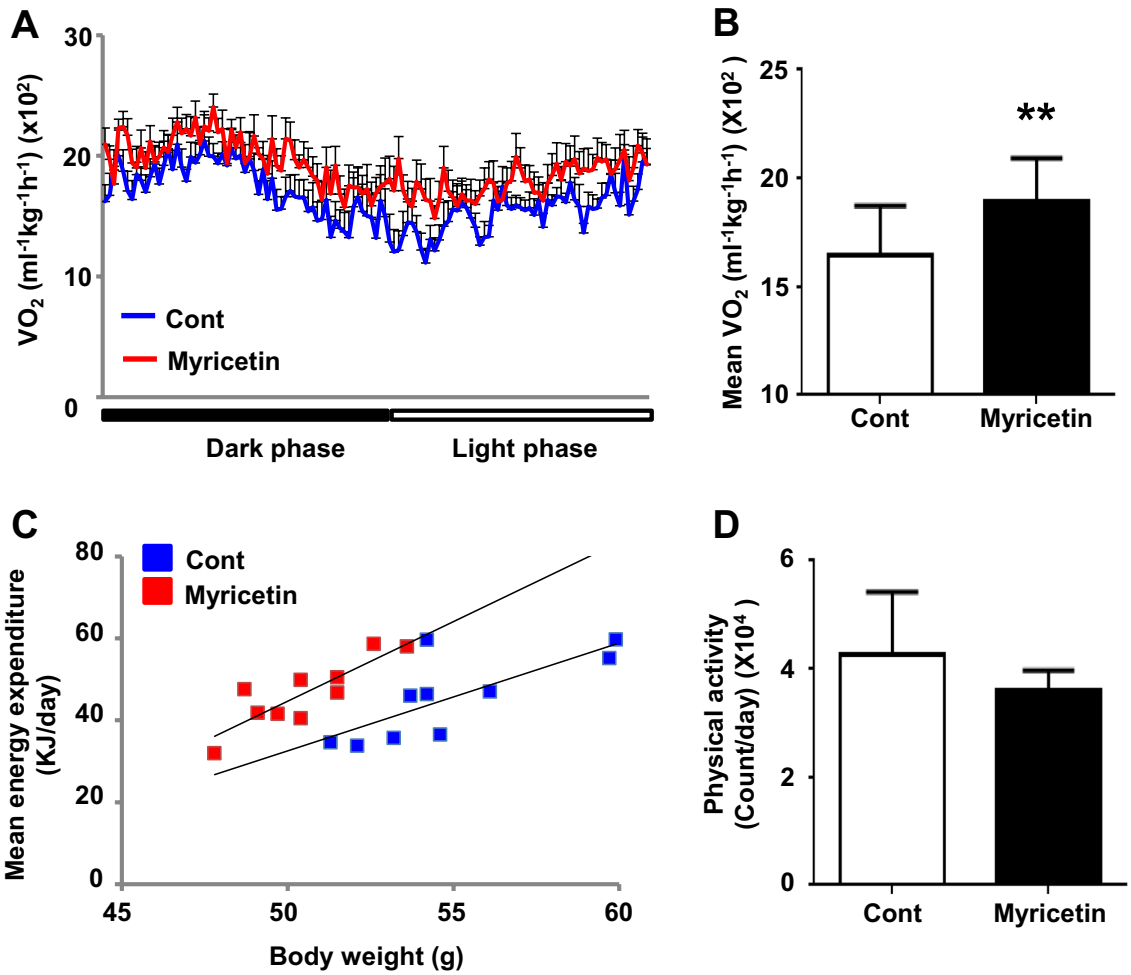

Fig. 3 Myricetin increases energy expenditure in db/db mice. Oxygen consumption was measured at 10 weeks after vehicle or myricetin treatment ($N = 10$/group) (**a**). Oxygen consumption (**b**) and mean energy expenditure (**c**) after vehicle or myricetin treatment. Spontaneous physical activity was measured by cumulative ambulatory counts for 24 h (**d**). A *graph* and *bars* represent means ± SD. **P < 0.01 vs Cont

acquired immediately after cold exposure also showed that myricetin-treated mice had higher skin temperature (Fig. 4c). These results support that myricetin activates BAT and thereby increases NST in db/db mice.

Myricetin activates thermogenic gene expression in BAT of db/db mice

Since myricetin induced BAT activation, we analyzed the protein level of thermogenic genes such as PGC1-α, UCP1 and mitochondrial oxidative phosphorylation (OXPHOS) in BAT from vehicle or myricetin-treated db/db mice. UCP1 and OXPHOS-related protein (ATP5A, UQCR2 and SDHB) expressions were significantly higher in myricetin-treated db/db mice (Fig. 5a, b). Consistently, immunohistochemical staining result reflected UCP1 upregulation in BAT from myricetin-treated db/db mice than control mice (Fig. 5c). Myricetin also increased mtDNA copy number (Fig. 5d) and the expression levels of SIRT1 and PGC1α that are involved in modulating mitochondrial biogenesis (Fig. 5a, b). Since NST is mainly regulated by sympathetic nervous system and thyroid hormone [31, 32], we analyzed the expression levels of tyrosine hydroxylase (TH) that converts phenylalanine into dopamine and iodothyronine deiodinase types 2 (dio2), which is the enzyme responsible for the conversion of T4 to T3. Both TH and Dio2 expressions in BAT were all increased significantly after myricetin treatment (Fig. 5e). Collectively, these results indicate that myricetin-mediated mitochondrial biogenesis is associated with sympathetic nervous system and thyroid hormone, leading to the activation of BAT.

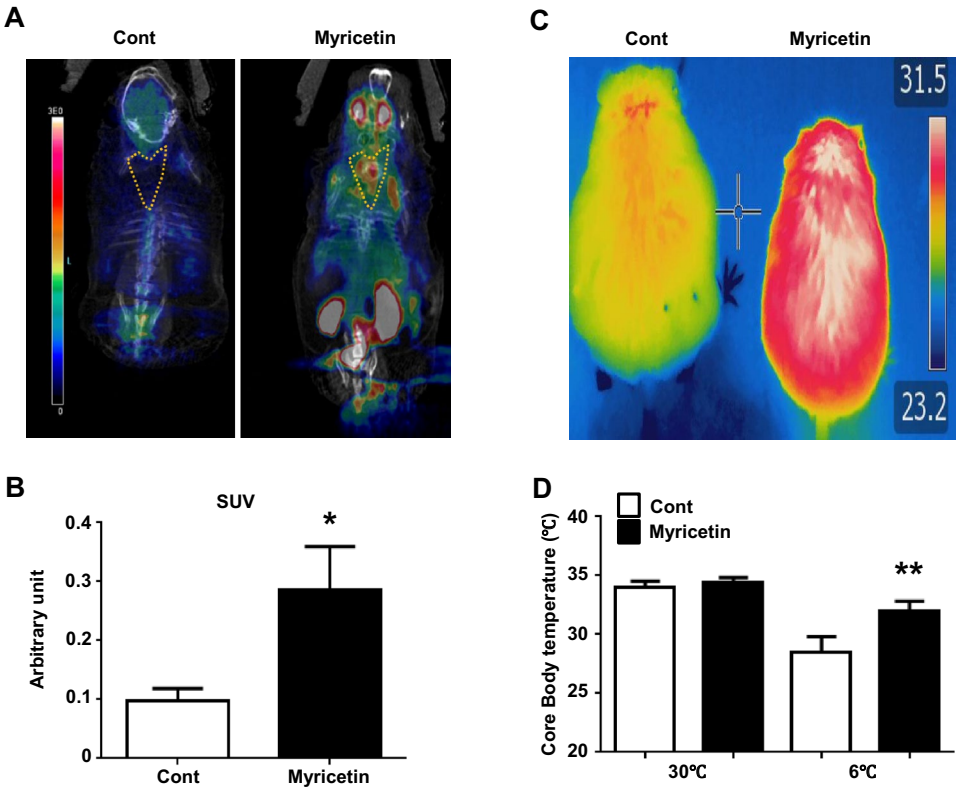

Fig. 4 Myricetin increases BAT activity and thermogenesis of db/db mice. Representative PET/CT images of vehicle or myricetin-treated db/db mice ($n = 5$/group) at 12 weeks after vehicle or myricetin treatment. *Yellow dashed triangle* represented the anatomical site of interscapular BAT (**a**). *Bar graph* represents mean uptake of ^{18}F-FDG in BAT (**b**). Representative infrared thermal image after cold exposure (**c**) at 13 weeks after vehicle or myricetin treatment. After 4 h of exposure to cold (6 °C), core body temperature of vehicle or myricetin-treated db/db mice was measured ($n = 10$/group) (**d**). *Bars* represent means ± SD. $^{*}P < 0.05$, $^{**}P < 0.01$ vs Cont

Myricetin induces beige formation of iWAT

Since NST also induces beige formation in iWAT [33], we identified whether myricetin induces browning in iWAT. Interestingly, the expression levels of beige cell-specific maker genes such as TBX1, CD137 and TMEM26 were significantly upregulated (Fig. 6a) with a higher induction of mitochondria biogenesis regulation genes (UCP1, PGC1-α and OXPHOS) at protein level after myricetin treatment (Fig. 6b–d) [34]. mtDNA copy number (Fig. 6e), the protein expression of SIRT1 and PGC1α (Fig. 6b, c), and the expression level of TH and Dio2 (Fig. 6f) were all significantly increased in iWAT from myricetin-treated db/db mice. However, plasma T3 and T4 concentration were not altered after myricetin treatment (Suppl. Figure 1), suggesting that dio2 was locally expressed in BAT and iWAT. These results indicate that myricetin induces beige formation in iWAT.

Myricetin directly regulates thermogenic program and adiponectin expression in brown adipocytes

To investigate whether myricetin directly regulates mitochondrial biogenesis in brown adipocytes, myricetin was introduced during differentiation of murine $C_3H_{10}T_{1/2}$ mesenchymal stem cell into brown adipocytes. Interestingly, differentiated brown adipocytes with myricetin expressed significantly higher mitochondria biogenesis regulation genes (UCP1 and PRDM16) than that with vehicle (Fig. 7a, b). Activated brown adipocytes express adiponectin that enhances lipid oxidation and improves insulin action [11–13, 35]. We, therefore, investigated whether myricetin effects on adiponectin expression in differentiated brown adipocytes. Surprisingly, myricetin upregulated the expression level of adiponectin in differentiated brown adipocytes (Fig. 7c) and the concentration of secreted adiponectin in culture media was also increased (Fig. 7d). For further evaluation, we analyzed the expression level of adiponectin in BAT, epididymal WAT and iWAT from vehicle or myricetin-treated db/db mice. In all three fat pads, adiponectin expression was increased after myricetin treatment (Fig. 7e). In addition, the concentration of adiponectin was significantly higher in plasma from myricetin-treated db/db mice than vehicle-treated db/db mice (Fig. 7f). In agreement with the data of Choi et al. [22], plasma level of TNFα that has a negative correlation with adiponectin was decreased after myricetin treatment.

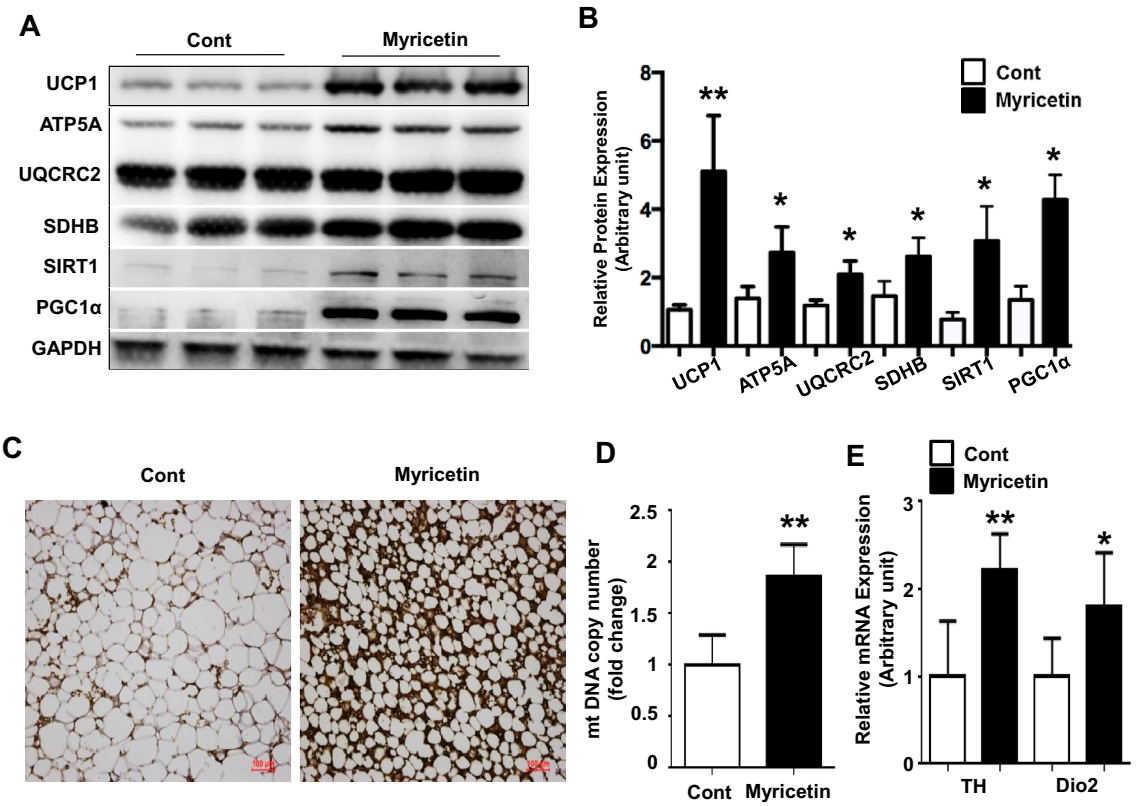

Fig. 5 Myricetin increases thermogenic gene expression in BAT. BAT was harvested from mice at 14 weeks after vehicle or myricetin treatment. Protein level of thermogenic genes and OXPHOS expression in BAT (**a, b**). Representative histologic images of UCP1-stained BAT (**c**). mtDNA copy number of BAT from db/db mice treated with vehicle or myricetin ($n=10$) (**d**). The relative mRNA expression of TH and Dio2 in BAT (**e**). *Bars* represent means ± SD. $^{*}P<0.05$, $^{**}P<0.01$ vs cont

Discussion

In current study, we showed that 14 weeks of myricetin treatment improved obesity and insulin resistance with the reduction of hepatic steatosis in db/db mice. In addition, we revealed that the beneficial effects of myricetin in db/db mice were associated with BAT activation and beige formation in iWAT. To the best of our knowledge, this is the first study that shows myricetin induces BAT activation and beige formation in WAT. Our result points out that myricetin-induced BAT activation may be a new therapeutic strategy for the treatment of obesity and its related metabolic syndromes.

Myricetin treatment decreases body weight gain and adipose tissue mass and prevents IR in high-fat and high-sucrose diet-induced obese mouse [22]. Consistently, body weight and fat mass were significantly reduced in db/db mice after myricetin treatment in our study (Fig. 1a, b). In addition, the size of adipocyte in BAT and iWAT (Fig. 1d, e) was smaller after myricetin treatment. Since diet consumption (Fig. 1c) and physical activity (Fig. 3d) were comparable between groups, the suppression of body weight gain may result from the reduction of adiposity. Additionally, myricetin-treated db/db mice showed higher oxygen consumption without a change in physical activity than vehicle-treated mice (Fig. 3a–d), suggesting that myricetin increased energy expenditure in db/db mice. BAT and beige formation are tightly associated with energy expenditure [6]. It is estimated that BAT mass range from ~30 to 300 g in human contributes to 20% of daily resting energy expenditure (REE) [14, 36] and activated BAT of small mammals to protect against cold environment increases energy expenditure by dissipating heat through NST [37]. Notably, myricetin increased the protein expression levels of UCP1 and mitochondrial oxidative phosphorylation (OXPHOS) in BAT (Fig. 5a–c) and iWAT (Fig. 6b–d). Sirt1 regulates mitochondrial biogenesis through deacetylation and activation of PGC-1α that interacts with the respiratory factors (NRF-1 and NRF-2), thereby inducing the transcription of mitochondrial biogenesis-related genes [38, 39]. Myricetin increased mtDNA copy number with a higher induction of Sirt1 and PGC-1α at the protein level in BAT (Fig. 5a, b, d) and iWAT (Fig. 6b, c, e),

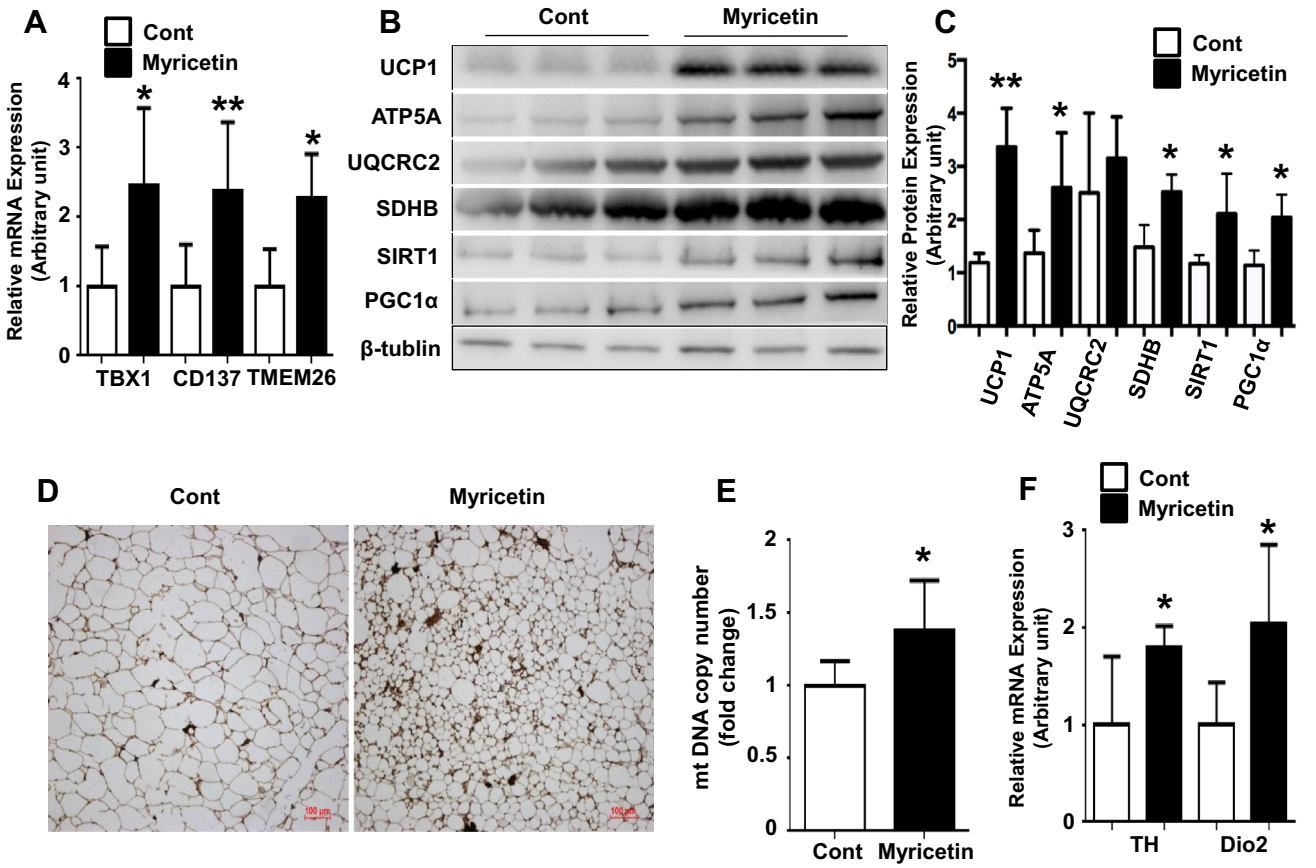

Fig. 6 Myricetin induces browning and thermogenic gene expression in iWAT. iWAT was harvested from mice at 14 weeks after vehicle or myricetin treatment. The relative mRNA expression of beige cell-specific markers in iWAT (**a**). Protein level of thermogenic genes and OXPHOS expression in BAT (**b, c**). Representative histologic images of UCP1-stained iWAT (**d**). mtDNA copy number of iWAT from db/db mice treated with vehicle or myricetin ($n = 10$) (**e**). The relative mRNA expression of TH and Dio2 in BAT (**f**). *Bars* represent means ± SD. $^{*}P < 0.05$, $^{**}P < 0.01$ vs Cont

suggesting that myricetin treatment could increase mitochondrial biogenesis and thereby result in the improvement of energy expenditure and thermogenesis. Furthermore, PET/CT image supported that BAT of db/db mouse was activated after myricetin treatment (Fig. 4a, b) and core body temperature and skin temperature were higher in myricetin-treated db/db mice than vehicle-treated mice after cold exposure (Fig. 4c, d). These results indicate that myricetin-mediated BAT activation and beige formation accounted for the improvement of energy expenditure in db/db mice. Consequently, myricetin improved insulin sensitivity (Fig. 2a, d), plasma lipid profiles (Table 1) and hepatic steatosis (Fig. 2e), since activated BAT promotes clearance of excessive triglycerides in the plasma by increasing lipid uptake into BAT, subsequently improving energy metabolism and weight loss [40, 41]. NST is mainly regulated by sympathetic nervous system and thyroid hormone [31, 32]. The expression levels of TH and DiO2 were upregulated in BAT (Fig. 5e) and iWAT (Fig. 6f) after myricetin treatment, indicating that both sympathetic nervous system and thyroid hormone may contribute to NST in myricetin-treated mice. Recently, our group reported that adiponectin expressed in the intact BAT after BAT transplantation ameliorates hyperglycemia, insulin sensitivity and energy expenditure through autocrine and/or endocrine mechanisms in obese mice [11–13]. Interestingly, adiponectin mRNA expression was upregulated in differentiated brown adipocyte and secreted adiponectin from differentiated brown adipocytes was increased after myricetin treatment (Fig. 7c, d). Adiponectin expression at the mRNA level was significantly increased in BAT, eWAT and iWAT after myricetin treatment (Fig. 7e) and plasma adiponectin concentration was higher in myricetin-treated mice than vehicle-treated mice (Fig. 7f). These results may indicate that myricetin directly regulated adiponectin expression in brown adipocyte by unknown mechanism and myricetin-mediated adiponectin expression could be

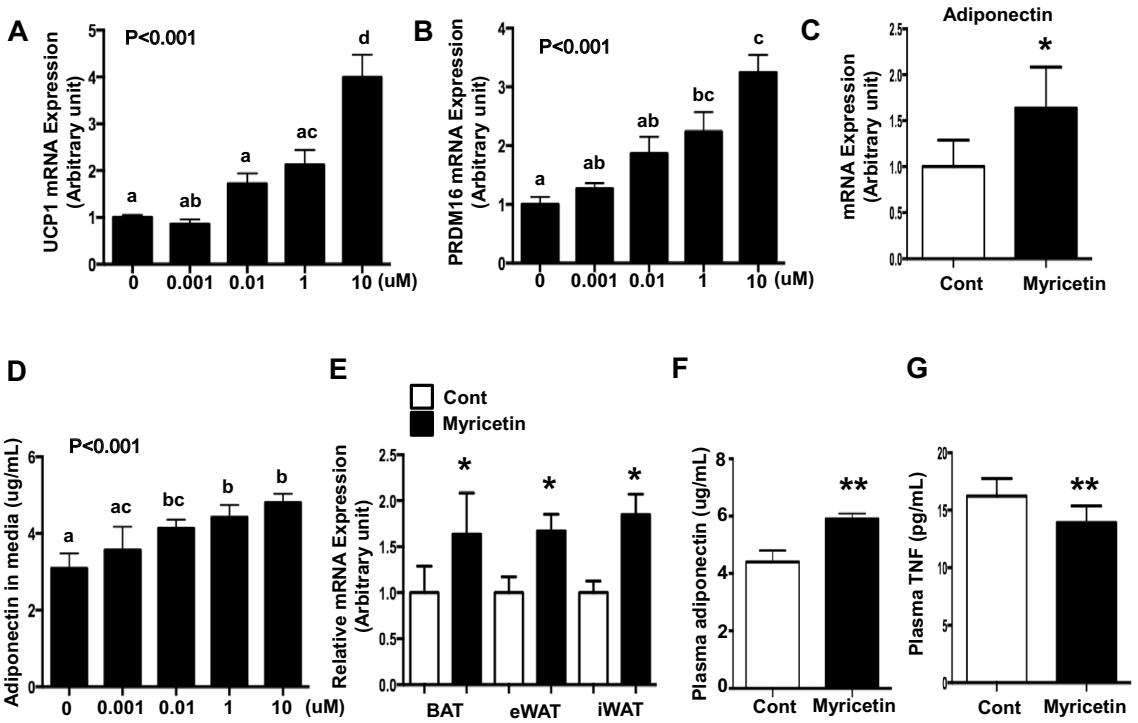

Fig. 7 Myricetin regulates thermogenic gene and adiponectin gene expression in $C_3H_{10}T_{1/2}$ cells. The relative mRNA expression of UCP1 in $C_3H_{10}T_{1/2}$ after myricetin treatment (**a**). The relative mRNA expression of PRDM16 in $C_3H_{10}T_{1/2}$ after myricetin treatment (**b**). The relative mRNA expression of adiponectin in $C_3H_{10}T_{1/2}$ after myricetin treatment (**c**). The concentration of adiponectin in culture media from $C_3H_{10}T_{1/2}$ after myricetin treatment (**d**). The relative mRNA expressions of adiponectin in BAT, eWAT and iWAT from myricetin- or vehicle-treated db/db mice (**e**). Plasma adiponectin concentration from vehicle- or myricetin-treated db/db mice (**f**). Plasma TNF concentration from vehicle- or myricetin-treated db/db mice (**g**). *Bars* represent means ± SD. Data analyzed by one-way ANOVA with Turkey's post hoc tests and different letters indicate significant differences among myricetin concentrations (**a, b, d**). $^{*}P < 0.05$, $^{**}P < 0.01$ vs Cont

another underlying mechanism for the improvement of obesity and systemic IR in db/db mice. Future studies are required to elucidate the contribution of myricetin to the induction of adiponectin in brown adipocytes. Also establishing the safety of chronic supplementation with high levels of myricetin should be tested in human for the therapeutic purpose. Collectively, our results in this study show that myricetin prevents obesity and systemic IR in db/db mice by activating BAT, recruiting beige cells and increasing adiponectin secretion in BAT.

Acknowledgements The authors declare that they have no conflict of interest. W.J., H.J.L. and H.L. designed the experiments. T.H., X.Y. and G.W performed the experiments and analyzed the data. W.J., H.J.L. and H.L. interpreted the data and wrote or revised the manuscript. All authors have approved the final version of the manuscript and agree to be accountable for all aspects of the work. All persons designated as authors qualify for authorship, and all those who qualify for authorship are listed. This work was supported by the Strategic Priority Research Program (XDB13030000), National Program on Key Basic Research Project (973 Program), the Ministry of Science and Technology of China (2015CB943102, 2012CBA01301 and 2012CB944701, respectively) and the National Natural Science Foundation of China (81370951 and 81600658).

References

1. Jensen MD, Ryan DH, Apovian CM, Ard JD, Comuzzie AG, Donato KA, Hu FB, Hubbard VS, Jakicic JM, Kushner RF, Loria CM, Millen BE, Nonas CA, Pi-Sunyer FX, Stevens J, Stevens VJ, Wadden TA, Wolfe BM, Yanovski SZ (2014) 2013 AHA/ACC/TOS guideline for the management of overweight and obesity in adults: a report of the American College of Cardiology/American Heart Association Task Force on Practice Guidelines and The Obesity Society. J Am Coll Cardiol 63 (25 Pt B):2985–3023. doi:10.1016/j.jacc.2013.11.004
2. Flegal KM, Kit BK, Orpana H, Graubard BI (2013) Association of all-cause mortality with overweight and obesity using standard body mass index categories: a systematic review and meta-analysis. Jama 309(1):71–82. doi:10.1001/jama.2012.113905
3. Solas M, Milagro FI, Martinez-Urbistondo D, Ramirez MJ, Martinez JA (2016) Precision obesity treatments including pharmacogenetic and nutrigenetic approaches. Trends Pharmacol Sci 37(7):575–593. doi:10.1016/j.tips.2016.04.008
4. Virtanen KA, Lidell ME, Orava J, Heglind M, Westergren R, Niemi T, Taittonen M, Laine J, Savisto NJ, Enerback S, Nuutila P (2009) Functional brown adipose tissue in healthy adults. N Engl J Med 360(15):1518–1525. doi:10.1056/NEJMoa0808949
5. van Marken Lichtenbelt WD, Vanhommerig JW, Smulders NM, Drossaerts JM, Kemerink GJ, Bouvy ND, Schrauwen P, Teule GJ (2009) Cold-activated brown adipose tissue in healthy men. N Engl J Med 360(15):1500–1508. doi:10.1056/NEJMoa0808718

6. Sidossis L, Kajimura S (2015) Brown and beige fat in humans: thermogenic adipocytes that control energy and glucose homeostasis. J Clin Invest 125(2):478–486. doi:10.1172/JCI78362
7. Schulz TJ, Tseng YH (2009) Emerging role of bone morphogenetic proteins in adipogenesis and energy metabolism. Cytokine Growth Factor Rev 20(5–6):523–531. doi:10.1016/j.cytogfr.2009.10.019
8. Gesta S, Tseng YH, Kahn CR (2007) Developmental origin of fat: tracking obesity to its source. Cell 131(2):242–256. doi:10.1016/j.cell.2007.10.004
9. Kim SH, Plutzky J (2016) Brown fat and browning for the treatment of obesity and related metabolic disorders. Diabetes Metab J 40(1):12–21. doi:10.4093/dmj.2016.40.1.12
10. Hankir MK, Cowley MA, Fenske WK (2016) A BAT-centric approach to the treatment of diabetes: turn on the brain. Cell Metab 24(1):31–40. doi:10.1016/j.cmet.2016.05.003
11. Liu X, Zheng Z, Zhu X, Meng M, Li L, Shen Y, Chi Q, Wang D, Zhang Z, Li C, Li Y, Xue Y, Speakman JR, Jin W (2013) Brown adipose tissue transplantation improves whole-body energy metabolism. Cell Res 23(6):851–854. doi:10.1038/cr.2013.64
12. Liu X, Wang S, You Y, Meng M, Zheng Z, Dong M, Lin J, Zhao Q, Zhang C, Yuan X, Hu T, Liu L, Huang Y, Zhang L, Wang D, Zhan J, Jong Lee H, Speakman JR, Jin W (2015) Brown adipose tissue transplantation reverses obesity in Ob/Ob Mice. Endocrinology 156(7):2461–2469. doi:10.1210/en.2014-1598
13. Yuan X, Hu T, Zhao H, Huang Y, Ye R, Lin J, Zhang C, Zhang H, Wei G, Zhou H, Dong M, Zhao J, Wang H, Liu Q, Lee HJ, Jin W, Chen ZJ (2016) Brown adipose tissue transplantation ameliorates polycystic ovary syndrome. Proc Natl Acad Sci USA. doi:10.1073/pnas.1523236113
14. Cypess AM, Lehman S, Williams G, Tal I, Rodman D, Goldfine AB, Kuo FC, Palmer EL, Tseng Y, Doria A, Kolodny GM, Kahn CR (2009) Identification and importance of brown adipose tissue in adult humans. N Engl J Med 360(15):1509–1517
15. Ohno H, Shinoda K, Spiegelman BM, Kajimura S (2012) PPARgamma agonists induce a white-to-brown fat conversion through stabilization of PRDM16 protein. Cell Metab 15(3):395–404. doi:10.1016/j.cmet.2012.01.019
16. Shabalina IG, Petrovic N, de Jong JM, Kalinovich AV, Cannon B, Nedergaard J (2013) UCP1 in brite/beige adipose tissue mitochondria is functionally thermogenic. Cell Rep 5(5):1196–1203. doi:10.1016/j.celrep.2013.10.044
17. Min SY, Kady J, Nam M, Rojas-Rodriguez R, Berkenwald A, Kim JH, Noh HL, Kim JK, Cooper MP, Fitzgibbons T, Brehm MA, Corvera S (2016) Human 'brite/beige' adipocytes develop from capillary networks, and their implantation improves metabolic homeostasis in mice. Nat Med 22(3):312–318. doi:10.1038/nm.4031
18. Miean KH, Mohamed S (2001) Flavonoid (myricetin, quercetin, kaempferol, luteolin, and apigenin) content of edible tropical plants. J Agric Food Chem 49(6):3106–3112
19. Semwal DK, Semwal RB, Combrinck S, Viljoen A (2016) Myricetin: a dietary molecule with diverse biological activities. Nutrients 8(2):90. doi:10.3390/nu8020090
20. Ong KC, Khoo HE (2000) Effects of myricetin on glycemia and glycogen metabolism in diabetic rats. Life Sci 67(14):1695–1705
21. Kandasamy N, Ashokkumar N (2014) Protective effect of bioflavonoid myricetin enhances carbohydrate metabolic enzymes and insulin signaling molecules in streptozotocin-cadmium induced diabetic nephrotoxic rats. Toxicol Appl Pharmacol 279(2):173–185. doi:10.1016/j.taap.2014.05.014
22. Choi HN, Kang MJ, Lee SJ, Kim JI (2014) Ameliorative effect of myricetin on insulin resistance in mice fed a high-fat, high-sucrose diet. Nutr Res Pract 8 (5):544–549. doi:10.4162/nrp.2014.8.5.544
23. Guo J, Meng Y, Zhao Y, Hu Y, Ren D, Yang X (2015) Myricetin derived from Hovenia dulcis Thunb. ameliorates vascular endothelial dysfunction and liver injury in high choline-fed mice. Food Funct 6 (5):1620–1634. doi:10.1039/c4fo01073f
24. Chi QS, Wang DH (2011) Thermal physiology and energetics in male desert hamsters (Phodopus roborovskii) during cold acclimation. J Comp Physiol B 181(1):91–103. doi:10.1007/s00360-010-0506-6
25. Chen HC, Farese RV Jr (2002) Determination of adipocyte size by computer image analysis. J Lipid Res 43(6):986–989
26. Livak KJ, Schmittgen TD (2001) Analysis of relative gene expression data using real-time quantitative PCR and the 2(-Delta Delta C(T)) method. Methods 25(4):402–408. doi:10.1006/meth.2001.1262
27. Seale P, Kajimura S, Yang W, Chin S, Rohas LM, Uldry M, Tavernier G, Langin D, Spiegelman BM (2007) Transcriptional control of brown fat determination by PRDM16. Cell Metab 6(1):38–54. doi:10.1016/j.cmet.2007.06.001
28. Wang B, Chandrasekera PC, Pippin JJ (2014) Leptin- and leptin receptor-deficient rodent models: relevance for human type 2 diabetes. Curr Diabetes Rev 10(2):131–145
29. de Luca C, Kowalski TJ, Zhang Y, Elmquist JK, Lee C, Kilimann MW, Ludwig T, Liu SM, Chua SC Jr (2005) Complete rescue of obesity, diabetes, and infertility in db/db mice by neuron-specific LEPR-B transgenes. J Clin Invest 115(12):3484–3493. doi:10.1172/jci24059
30. Rosen ED, Spiegelman BM (2014) What we talk about when we talk about fat. Cell 156(1–2):20–44. doi:10.1016/j.cell.2013.12.012
31. Himms-Hagen J (1984) Nonshivering thermogenesis. Brain Res Bull 12(2):151–160
32. Ribeiro MO, Carvalho SD, Schultz JJ, Chiellini G, Scanlan TS, Bianco AC, Brent GA (2001) Thyroid hormone–sympathetic interaction and adaptive thermogenesis are thyroid hormone receptor isoform–specific. J Clin Invest 108(1):97–105. doi:10.1172/jci12584
33. Cohen P, Spiegelman BM (2015) Brown and beige fat: molecular parts of a thermogenic machine. Diabetes 64(7):2346–2351. doi:10.2337/db15-0318
34. Wu J, Bostrom P, Sparks LM, Ye L, Choi JH, Giang AH, Khandekar M, Virtanen KA, Nuutila P, Schaart G, Huang K, Tu H, van Marken Lichtenbelt WD, Hoeks J, Enerback S, Schrauwen P, Spiegelman BM (2012) Beige adipocytes are a distinct type of thermogenic fat cell in mouse and human. Cell 150(2):366–376. doi:10.1016/j.cell.2012.05.016
35. Yamauchi T, Kamon J, Waki H, Terauchi Y, Kubota N, Hara K, Mori Y, Ide T, Murakami K, Tsuboyama-Kasaoka N, Ezaki O, Akanuma Y, Gavrilova O, Vinson C, Reitman ML, Kagechika H, Shudo K, Yoda M, Nakano Y, Tobe K, Nagai R, Kimura S, Tomita M, Froguel P, Kadowaki T (2001) The fat-derived hormone adiponectin reverses insulin resistance associated with both lipoatrophy and obesity. Nat Med 7(8):941–946. doi:10.1038/90984
36. Carey AL, Kingwell BA (2013) Brown adipose tissue in humans: therapeutic potential to combat obesity. Pharmacol Ther 140(1):26–33. doi:10.1016/j.pharmthera.2013.05.009
37. Bi S, Li L (2013) Browning of white adipose tissue: role of hypothalamic signaling. Ann N Y Acad Sci 1302:30–34. doi:10.1111/nyas.12258
38. Price NL, Gomes AP, Ling AJ, Duarte FV, Martin-Montalvo A, North BJ, Agarwal B, Ye L, Ramadori G, Teodoro JS, Hubbard BP, Varela AT, Davis JG, Varamini B, Hafner A, Moaddel R, Rolo AP, Coppari R, Palmeira CM, de Cabo R, Baur JA, Sinclair DA (2012) SIRT1 is required for AMPK activation and the beneficial effects of resveratrol on mitochondrial function. Cell Metab 15(5):675–690. doi:10.1016/j.cmet.2012.04.003

39. Scarpulla RC (2011) Metabolic control of mitochondrial biogenesis through the PGC-1 family regulatory network. Biochim Biophys Acta 1813(7):1269–1278. doi:10.1016/j.bbamcr.2010.09.019
40. Bartelt A, Bruns OT, Reimer R, Hohenberg H, Ittrich H, Peldschus K, Kaul MG, Tromsdorf UI, Weller H, Waurisch C, Eychmuller A, Gordts PL, Rinninger F, Bruegelmann K, Freund B, Nielsen P, Merkel M, Heeren J (2011) Brown adipose tissue activity controls triglyceride clearance. Nat Med 17(2):200–205. doi:10.1038/nm.2297
41. Yoneshiro T, Aita S, Matsushita M, Kayahara T, Kameya T, Kawai Y, Iwanaga T, Saito M (2013) Recruited brown adipose tissue as an antiobesity agent in humans. J Clin Invest 123(8):3404–3408. doi:10.1172/jci67803